Novel 3-D macrophage spheroid model reveals reciprocal regulation of immunomechanical stress and mechano-immunological response

Alice Burchett[1], Saeed Siri[1], Jun Li[2], Xin Lu[3], and Meenal Datta[1,*]

[1]Department of Aerospace and Mechanical Engineering, University of Notre Dame, IN, USA
[2]Department of Applied and Computational Mathematics and Statistics, University of Notre Dame, IN, USA
[3]Department of Biological Sciences, University of Notre Dame, IN, USA
* Address correspondence to: mdatta@nd.edu

Abstract

Purpose: In many diseases, an overabundance of macrophages contributes to adverse outcomes. While numerous studies have compared macrophage phenotype after mechanical stimulation or with varying local stiffness, it is unclear if and how macrophages themselves contribute to mechanical forces in their microenvironment.

Methods: Raw 264.7 murine macrophages were embedded in a confining agarose gel, where they proliferated to form spheroids over time. Gels were synthesized at various concentrations to tune the stiffness and treated with various growth supplements to promote macrophage polarization. The spheroids were then analyzed by immunofluorescent staining and qPCR for markers of proliferation, mechanosensory channels, and polarization. Finally, spheroid geometries were used to computationally model the strain generated in the agarose by macrophage spheroid growth.

Results: Macrophages form spheroids and generate growth-induced mechanical forces (i.e., solid stress) within confining agarose gels, which can be maintained for at least 16 days in culture. Increasing agarose concentration restricts spheroid expansion, promotes discoid geometries, limits gel deformation, and induces an increase in iNOS expression. LPS stimulation increases spheroid growth, though this effect is reversed with the addition of IFN-γ. Ki67 expression decreases with increasing agarose concentration, in line with the growth measurements.

Conclusions: Macrophages alone both respond to and generate solid stress. Understanding how macrophage generation of growth-induced solid stress responds to different environmental conditions will help to inform treatment strategies for the plethora of diseases that involve macrophage accumulation.

Keywords: solid stress, inflammation, microenvironment, myeloid cells, polarization

Acknowledgments

Funding for this work was provided by the National Institutes of Health (NIH/NCI K22CA258410 and NIH/NIGMS R35GM151041), the Indiana Clinical Sciences and Translational Institute, and the Berthiaume Institute for Precision Health (all to M.D.). Other funding support included National Institutes of Health grants R01CA248033 (to X.L.) and R01CA280097 (to X.L., J.L.) and Department of Defense grants W81XWH2010312, W81XWH2010332, HT94252310010 and HT94252310613 (to X.L.). Histology was performed at the Notre Dame Histology Core, and multiphoton imaging was performed at the Notre Dame Integrated Imaging Facility, with the assistance of Dr. Sara Cole. The authors thank Ms. R'nld Rumbach for technical assistance, and Prof. Donny Hanjaya-Putra and his laboratory for imaging assistance.

Statements and Declarations

Competing Interests: The authors have no financial or non-financial interests to disclose.

Author Contributions

M.D. and A.B. conceived of and designed this study, A.B. performed experiments and analysis of experimental data, S.S. performed computational analyses, data curation and image processing, A.B., S.S., J.L., X.L., M.D. contributed to data analysis and interpretation, A.B., S.S., and M.D. wrote the manuscript, and all authors reviewed and approved the final version.

Introduction

From atherosclerotic plaques to solid cancerous tumors, macrophages play important roles in immune effector function and orchestration, and as active constituents of the mechanical microenvironment [1]. As innate immune cells, they are not only part of the first line of defense against pathogens, they also contribute to tissue repair and help coordinate the broader immune response. Macrophage phenotype is highly plastic and ebbs between pro- and anti-inflammatory states, as these cells sense and correspondingly respond to diverse and dynamic microenvironments [2]. Macrophages present in tissues are either resident or derived from circulating monocytes that differentiate into macrophages upon vascular extravasation and tissue penetration [3]. During an inflammatory response, an injured or diseased site will accumulate macrophages, both through the recruitment of circulating monocytes and local proliferation of bone marrow and embryonic-derived macrophages [4]. For example, upon tissue injury, vascular endothelial cells upregulate adhesion molecules that allow patrolling monocytes to adhere to the vessel wall, where they withstand shear stress from blood flow, and eventually enter the tissue between endothelial junctions [5].

While macrophage phenotype and function, known also as polarization, is traditionally thought to be either pro-inflammatory (“M1-like”) or anti-inflammatory (“M2-like”), their dynamic cell state can lie on a continuum between inflammation-accelerating and inflammation-inhibiting responses [6]. Macrophages adopt and shift between these polarizations in any tissue; generally, equilibrium between the two ends of the spectrum is essential for homeostatic tissue maintenance and repair. However, an over- or under-active macrophage response can disrupt this tenuous balance, particularly in cases where macrophages accumulate in large quantities.

Elevated macrophage populations in diseased tissue are often correlated with worse prognosis, particularly in diseases where altered tissue mechanics contribute to the pathophysiology [7]. Cancer, wound healing, bacterial infections, and other disease settings involve altered tissue mechanics, which impact immune surveillance [8]. For example, atherosclerotic plaques physically disrupt blood flow, and their mechanical stability determines if they will rupture, leading to downstream ischemic events [9]. Macrophages accumulate in plaques, where they contribute to this mechanical instability, increasing the risk of life-threatening events such as a stroke. Macrophages infiltrate tumor microenvironments in high numbers, with the density of tumor-associated macrophages correlating with worse prognoses in cancers including glioblastoma, ovarian cancer, and breast cancer [10–14]. In glioblastoma, macrophages can comprise up to 50% of the tumor bulk, promoting tumor progression and treatment resistance [15–17]. Macrophages also contribute to increased collagen deposition in hypertrophic scars and heart attack scarring, leading to diminished tissue function [18, 19].

In addition to classical biochemical cues, macrophages also respond to mechanical stimuli such as shear stress, tissue viscoelasticity, cyclic compression or stretching, and hydrodynamic pressure changes [20]. This response has been characterized in prior studies, particularly in the context of the cardiovascular and skeletomuscular systems [21–24]. Macrophages experience a wide range of tissue mechanical properties, with Young’s moduli on the order of single kilopascals in the brain to tens of gigapascals in bone [25, 26]. *In vitro* experiments show that macrophages have a stronger inflammatory response when cultured on stiffer 2-D substrates [27–31]. However, the opposite effect is observed when cells are cultured in a 3-D matrix. Macrophages in stiffer matrices *in vitro* and *in vivo* have a more immunosuppressive, M2-like phenotype [32–34]. Thus, a physiologically relevant *in vitro* model is essential to understanding how macrophages respond – and contribute – to mechanical stimuli in the body.

Studies on macrophage mechanical responses largely neglect the impact of growth-induced mechanical forces – including solid stress [35], generated by solid tissue components (cells and matrix) – on macrophage proliferation. Further, the degree to which macrophages directly contribute to mechanical stress through their physical presence, accumulation, and proliferation in tissue remains unexplored. Here, we aimed to characterize the solid stress that macrophages generate through 3-D growth in a confining agarose gel, simulating the mechanics of the tissue microenvironment independent of confounding biochemical cues or matrix degradation.

Macrophages (RAW264.7) were embedded in agarose gels of varying substrate concentrations to span a range of physiologically-relevant stiffnesses. As the agarose-embedded cells proliferated to form spheroids, they displaced the surrounding gel, in a similar manner to a cancerous tumor generating and exerting solid stress on the surrounding tissue [36]. Spheroids in softer gels reached much larger sizes and caused larger displacements of the surrounding gel compared to spheroids in stiffer gels. Pro-inflammatory stimulation with lipopolysaccharide

(LPS) also led to an increase in spheroid size, though this effect was reversed with the addition of IFNγ. The mechanosensitive ion channels Piezo1 and transient receptor potential vanilloid 4 (TRPV4) both decreased in trend with increased stiffness. Markers of both pro- and anti-inflammatory functional status both showed a trending increase with stiffness, though only the pro-inflammatory marker reached statistical significance. Overall, this work highlights a novel, tunable, and high throughput method of interrogating macrophage immunomechanics and mechano-immunology, with relevance to a wide range of diseases.

Materials and Methods

Cell culture, gel formation, and macrophage activation/polarization

RAW264.7 murine macrophages were purchased from ATCC (TIB-71). They were grown in a complete culture medium consisting of DMEM (Corning, 10-013-CV) supplemented with 10% Fetal Bovine Serum (Gibco, 26140079) and 1% penicillin-streptomycin (Corning, 30-002-CI). They were maintained in a humidified incubator at 37°C with 5% CO_2. Cells were grown as adherent monolayers and passaged using a cell scraper for mechanical detachment.

To create agarose-embedded 3-D cultures, single-cell suspensions were mixed with low-gelling temperature agarose (Sigma-Aldrich, A0701-25G). First, a 4% agarose solution was made in a complete culture medium and heated in a microwave until dissolved. The liquid agarose was maintained at 48°C until use. Single-cell suspensions of RAW264.7 cells in medium were made ranging between 1000 cells/mL to 10,000,000 cells/mL and mixed with a proportional amount of the 4% agarose to create gels of 0.5%, 1%, or 2% agarose. The cell-agarose solution was pipetted into 2 mm-deep cylindrical molds and left at room temperature to set for 10 minutes. The gels were then removed from the molds, submerged in culture medium, and maintained under standard culture conditions.

For macrophage-stimulation-treated gels, the medium was supplemented with 200 ng/ml LPS. For M1-polarization-treated gels, the medium was supplemented with 20 ng/ml IFN-γ (BioLegend, 575302) and 200 ng/ml LPS (Santa Cruz Biotechnology, Inc, sc-3535). For M2-polarization-treated gels, the medium was supplemented with 20 ng/ml IL-4 (Pepro-Tech, 214-14). The volume of the gel was included in the total solution volume to achieve the final concentrations. Gels cultured under hypoxic conditions were placed in a Tri-Gas hypoxia incubator with 5% CO_2 and 1% O_2. Compressed gels were placed on a 0.4 μm pore size transwell cell culture insert (CellQART, 9310402) and a 3-D printed PLA weight was placed on top to apply 0.15 kPa of compression to the gel to simulate the solid stress measured in murine glioblastoma models [17, 37, 38]. A 1% agarose cushion was placed between the cells and the weight to serve as a media reservoir and protect cells from direct contact with the rigid weight.

Staining whole agarose gels

For live/dead staining, the gels were incubated with 2 μg/ml Calcein-AM (BioLegend, 425201) and 1 μg/ml Propidium Iodide (MP Biomedicals, 0219545810) in complete medium for 30 minutes at 37°C. These were imaged on a point-scanning confocal microscope (Nikon AXR). To obtain 3-D images of the spheroids for strain quantification, the gels were fixed overnight in 4% paraformaldehyde in PBS (Thermo Fisher, J19943.K2) at 4°C, then rinsed with PBS and incubated with CellMask™ Orange Actin Tracking Stain (1:1000, Thermo Fisher, A57244) and DAPI (2 μg/ml Sigma-Aldrich, D9542) for 48 hours at 4°C. Image stacks were acquired using a multiphoton microscope (Leica Stellaris 8 DIVE).

Immunofluorescent staining

After fixation as described above, gels were immersed in 30% sucrose overnight at 4°C, then transferred to a 1:1 solution of 30% sucrose and OCT (VWR, 95057-838) overnight at 4°C. The gels were then frozen in OCT and sectioned into 5 μm thick slices. The sections were incubated with primary antibodies for Ki67 (1:100, Novus Biologicals, NB110-89719) or Piezo1 (1:100, Proteintech, 15939-1-AP) overnight at 4°C. The following day, the slides were incubated with an anti-rabbit secondary antibody (1:500, abcam, ab150077) and DAPI and imaged (Leica DMi8).

Image analysis

Spheroid contour plots were generated in Autodesk Inventor using surface files generated by ImageJ. For size comparison, spheroids were identified manually from brightfield images and analyzed using ImageJ's Analyze

Particles function. For immunofluorescent-stained sections, the spheroid area was identified by CellProfiler using the combined antibody and DAPI channels, and the average intensity within the spheroid area was recorded.

PCR

RNA was collected from agarose-embedded cells after 48 hours in culture. For each sample, a small piece of gel (~100 µl volume) was dissolved in 400 µl TRI-reagent (Zymo Research, R2050-1-200) and the RNA was purified using an RNA isolation kit (Zymo Research, R2051). Gene expression was analyzed using TaqMan primers for Piezo1 (Mm01241549_m1), TRPV4 (Mm00499025_m1), Ki67 (Mm01278617_m1), Caspase 3 (Mm01195085_m1), and GAPDH (Mm99999915_g1). Gene expression was normalized to GAPDH reported as $2^{-\Delta\Delta Ct}$.

Computational modeling

To investigate the distribution of solid stress around the spheroids, a computational modeling approach was employed using COMSOL Multiphysics. Agarose gels with concentrations of 0.5%, 1%, and 2% were modeled as linear elastic materials (E = 2000, 19830, and 99596 Pa respectively). The spheroid geometry was obtained through image processing techniques and subsequently implemented in COMSOL. The initial geometry of the spheroid was considered as a sphere with a 5-micrometer radius. Through the application of prescribed displacement boundary conditions, the spheroids were expanded to their final geometry within the agarose gel. This approach allowed for the exploration of the solid stress and displacement distribution around the spheroids. The modeling simulations were conducted in 2D, providing a comprehensive analysis of the mechanical stress distribution within the agarose gel environment. This methodological approach enables a detailed examination of the impact of agarose gel concentration on the mechanical behavior of macrophage spheroids in a controlled and reproducible manner.

Statistical Analysis

Statistical analyses and data visualization were done using Graphpad Prism. For spheroid viability and size analysis, datasets were compared using the Kruskall-Wallace one-way analysis of PCR data was compared with unpaired two-sample t-tests. variance Error bars indicate standard deviation, and asterisks indicate statistical significance (*p<0.05, **p<0.01, ***p<0.001, ****p<0.0001).

Results

Agarose-embedded macrophages form spheroids with long-term viability

To determine if macrophages alone can generate solid stress, we seeded single cells in an agarose hydrogel. As a plant-derived material, agarose is biologically inert to mammalian cells, and is also physically and chemically stable, with suitable biocompatibility [39, 40]. The mechanical properties of agarose are also easily tunable, as Young's modulus increases exponentially with molar concentration [41]. Based on previous mechanical characterization by others and our own unconfined compression testing, we estimate that the Young's moduli of 0.5%, 1%, and 2% agarose gels to be 2 kPa, 20 kPa, and 100 kPa, respectively [41]. These approximately correspond to the stiffness ranges measured in the brain, healthy heart, and fibrotic scar tissue, respectively [26, 42, 43] . Because the embedded macrophages cannot degrade the surrounding matrix, any cell growth must cause solid stress, as the cells must displace the elastic material in order to proliferate and form 3-D spheroids.

We observed that RAW264.7 murine macrophages readily form spheroids when embedded in agarose at concentrations between 0.5% and 2%. Gels with lower than 0.5% agarose content were excluded due to manipulation challenges. The majority of cells seeded in gels between 0.5% and 4% were still viable 24 hours after seeding, with the only significant difference being between 0.75% and 3% agarose, as quantified by calcein AM (i.e., live cells) and propidium iodide (i.e., dead cells) staining (**Fig. 1a**). However, gels with more than 2% agarose content failed to produce spheroids; thus 2% agarose was used as the maximum concentration condition. Agarose-embedded macrophage spheroids display excellent long-term viability, with live spheroids observed at least 16 days after seeding (**Fig. 1b**). The size and topography of these spheroids are sensitive to agarose gel concentration (**Fig. 1c**). This maximum time in culture was limited only by the over-proliferation of cells present on the gel surface or in the surrounding media, rather than those embedded within the gels, but it is likely these constructs could be maintained for much longer periods. Macrophages grown in 0.5% agarose grew notably faster than those in 1% agarose, which were correspondingly faster than those in 2% agarose. This effect was visible by eye as the aggregates became large enough to see over time. This was also apparent by the increased rate of media consumption in lower percentage gels.

Macrophages generate solid stress in confining agarose gels

3-D imaging reveals that many spheroids adopt a flattened discoid shape, rather than a spherical shape (**Fig. 2**). Because macrophages cannot alter the plant-derived agarose matrix, any increase in spheroid size must cause displacement of the surrounding gel, thereby generating solid stress. Given an estimate of the spheroid geometry and the mechanical properties of the gel, we generated a simulation of the stress field in the gel surrounding the spheroids (**Fig. 2a**). Simulations of spheroid displacement during growth are shown based on fluorescent images. In **Fig. 2b** from left to right, the first three simulations for a spheroid embedded in 0.5%, 1% and 2% agarose gels assume no microcrack developments in the gels and an initial uniformly spherical geometry with a 5 μm radius, while the simulation for the spheroid in the 2% agarose gel with a discoid shape assumes formation and propagation of a microcrack in the gel during initial spheroid growth. The greatest solid stress-induced deformations are observed in 0.5% gels (with maximum gel displacements of ~250 μm), compared to stiffer 2% gels with spherical (40 μm) and discoid (42 μm) shapes. However, solid stress propagates further into the surrounding matrix with increasing gel concentrations. These data demonstrate that increasing the rigidity of the surrounding agarose matrix by elevating gel concentration significantly restricts spheroid expansion and modulates growth morphology. The decreased gel displacement and altered shape in stiffer gels indicates that the increased mechanical resistance of the matrix impedes outward growth. In contrast, the more mechanically permissive and compliant 0.5% agarose gel allows for greater spheroid expansion which maintains a rounded shape.

Spheroid size decreases with increasing agarose concentration and increases with pro-inflammatory stimulation

Varying the concentration of agarose, as illustrated above, drastically impacts spheroid size without significantly altering viability within the range of 0.5% and 2% agarose, as determined by the ratio of propidium iodide-positive to calcein AM-positive cells. We also tested other biologically relevant stimuli, including addition of pro-inflammatory (M1-like) and anti-inflammatory (M2-like) polarizing cytokines, LPS stimulation, and hypoxic environments. For each of these conditions, we compared the spheroid area observed by brightfield microscopy. As agarose concentration decreases, the average spheroid size increases significantly (**Fig. 3a)**. In 0.5% agarose, spheroids are much less regular in shape than those in 1% and 2% as is apparent in images of fluorescently labeled actin at day 4 after seeding (**Fig. 3b**). Treating the agarose-embedded macrophages with 200 ng/ml LPS resulted in significantly increased spheroid size compared to untreated, for both 0.5% and 1% gels However, treatment with 20 ng/ml IFNγ in addition to 200 ng/ml LPS (i.e., M1-like polarization) decreased spheroid size. Treatment with 20 ng/ml of IL-4 (i.e., M2-like polarization) trended towards increased spheroid size. Interestingly, hypoxia did not significantly alter spheroid size.

Stiffer gels reduce proliferation and mechanosensing protein expression in spheroids

As apparent in **Fig, 3b**, macrophage spheroids do not grow equally in all directions depending on their microenvironmental conditions, resulting in large-scale irregularity (e.g., ellipticity), and cell-scale differences in boundary uniformity (i.e., solidity). While we assumed in the simulation in **Fig. 2b** that discoid morphology is mechanically-driven (e.g., by micro-crack formation in the agarose gels), an alternative hypothesis could be tested that the irregular shape is biologically-driven (e.g., by anistropic proliferation). Therefore, we opted for a histological approach to capture any spatial differences in relevant biological markers that could be driving the asymmetry. Ki67 staining intensity decreased with increasing agarose concentration (**Fig. 4a**), corresponding to the decrease in spheroid size quantified above (**Fig. 3a**). The distribution of Ki67 cells throughout the spheroid did not clearly favor an edge versus central position (**Fig. 4b**). This indicates that differential rates of growth in different spatial directions may not be the result of variations in proliferation. This suggests that there may be a purely mechanical driving force behind the observed discoid shapes, such as the formation of cracks in the agarose gel and propagation of the spheroid into the crack space.

We also stained Piezo1, a mechanosensitive ion channel known to be involved in mechanotransduction in myeloid cells [44, 45]. Expression was distributed throughout the spheroid, with a slight peak at the center (**Fig. 4b**). In 2% agarose, Piezo1 expression was diminished, with a statistically significant decrease in average intensity between 1% and 2% agarose conditions (**Fig. 4a**). This result contrasts with prior studies showing that Piezo1 expression increases with stiffness in 2-D culture [46]. Piezo1 is a stretch-activated channel, but because mammalian cells cannot bind to the agarose, increased stiffness would not directly cause increased traction forces that are known to activate Piezo1 [47]. Piezo1 activation has been shown to promote myeloid cell

expansion, so the concurrent increase in Piezo1 and Ki67 expression with reduced agarose concentration could be part of a causative relationship [44].

Macrophages in 3D gels display altered mechanical and inflammatory transcriptional responses to varied mechano-chemical stimuli

We next compared the transcriptional activity of macrophages in various conditions. *Ki67* decreased significantly between 1% to 2% agarose (**Fig. 5a**). This aligns well with the spheroid size data (**Fig 3a**), implicating reduced proliferation behind the observed reduced spheroid size in stiffer gels. *Casp3*, an apoptosis marker, increased between 1% and 2%, but not between 0.5% and 1%. So, apoptosis is likely not responsible for the reduced size with increased stiffness, at least between 1% and 2% gels. Externally applied compression also decreased *Ki67* expression. M1-like polarization, M2-like polarization, and LPS stimulation all significantly decreased both *Ki67* and *Casp3* expression.

In addition to *Piezo1*, we also quantified *Trpv4*, another stretch-activated ion channel known to be involved in myeloid mechanotransduction [31, 48, 49]. *Trpv4* expression decreased between 0.5% and 1% agarose, and decreased with both M1 and LPS treatments (**Fig. 5b**). *Piezo1* expression also decreased with both M1 and LPS treatment. This potentially indicates that a decreased sensitivity to confining solid stress may play a role in the increase observed spheroid size between untreated and LPS-treated gels (**Fig. 3a**). Finally, we quantified canonical markers of pro-inflammatory macrophage activation (*Nos2*) and anti-inflammatory polarization (*Arg1*) (**Fig. 5c**). We observed a significant increase in *Nos2* with increasing gel stiffness as well as a trend towards increased *Arg1* with increasing gel stiffness. As expected, *Nos2* increased with M1 and LPS treatment, and decreased with M2 treatment. However, *Arg1* unexpectedly increased with all three stimulation/polarization treatments, potentially indicating altered phenotypic response to these stimuli in 3-D compared to previously observed 2-D culture results.

Discussion

This 3-D model of macrophage spheroid formation and the accompanying computational modeling of stresses and strains and downstream cellular and molecular biology readouts on polarization combine to make a novel platform for investigating the immunomechanics and mechano-immunology of macrophages in varying biochemical and mechanical microenvironments. The agarose gel constructs are simple and inexpensive to create, making them attractive for high-throughput applications, such as drug screening. The model is also highly amenable to more complex co-culture or organoid experiments, as any number of cell types and treatments can be applied. It could therefore be used to model solid stress in other disease settings, such as within tumors or tuberculosis granulomas where macrophages dominate [50]. Additionally, the agarose gels can be processed identically to tissues for histological analysis. In this work, we cryopreserved the samples for immunofluorescent staining, but we have also successfully processed agarose-cell constructs for paraffin embedding and immunohistochemical staining. By increasing the density of cells initially seeded, we were also able to easily obtain sufficient RNA for multiple qPCR analyses.

To the best of our knowledge, this is the first demonstration of successful spheroid formation, long-term viability, and solid stress generation by macrophages alone. While many aspects of macrophage responses to various forms of mechanical stress have been studied, relatively little has been shown of the reciprocal regulation of macrophages and solid stress [7]. Our simulation results suggest that the mechanical microenvironment can override intrinsic growth programs to control spheroid expansion. Lower stiffness gels allow for a greater displacement of the gel around the spheroid compared to higher stiffness gels. However, in stiffer gels, the stress propagates further into the surrounding gel. This work also reveals an interesting 3-D growth pattern, as macrophages often adopt a flattened discoid shape, rather than a spheroidal shape. This could indicate either a physical process, such as the formation of a planar crack in the gel, or a biological process, such as differential proliferation or tip/leader cell migratory behavior in different regions of the spheroid [51]. Further work to characterize the agarose gel surrounding a spheroid and potential crack propagation is underway. A limitation of the computational model is that it provides an estimate of the displacement and solid stress of the agarose adjacent to the spheroid, but not within the spheroid itself. Future work to characterize the mechanical properties of macrophage spheroids would inform computational modeling of stress distribution within the spheroids.

The most potent biochemical cue that increases macrophage spheroid size and stress generation at all tested agarose concentrations is treatment with LPS, an immunostimulatory bacterial fragment used to mimic the effect of bacterial infection [52, 53]. Interestingly, the addition of IFNγ along with LPS, a standard M1-like polarizing regime, reversed the effect of LPS entirely. IFNγ and LPS are generally thought to synergize to induce an M1-like phenotype, but this 3-D stress-generation model seems to have identified a way in which the two oppose one another [54]. Further mechanistic studies utilizing this model will help to elucidate the nuances of LPS-stimulated versus canonically M1-like polarized macrophages. Prior studies have shown an inflammatory response when macrophages are cultured on stiffer 2-D substrates, but a more immunosuppressive phenotype when in a 3D matrix [27–34]. However, our results show an increase in an M1 marker with increased stiffness, indicating potential similarity with 2D observations.

In line with observations by others, TRPV4 expression decreased with stiffness as part of an M1-like response [31]. However, we also observed a large but not statistically significant increase in an M2 marker with stiffness. Piezo1 expression by macrophages has been shown to increase on stiffer surfaces [46, 55]. However, we observed a trend towards decreased Piezo expression with increased stiffness. Cells in a confining gel such as agarose that does not support cell adhesion may not experience the membrane tension that activates stretch-activated channels such as Piezo1 [56]. Further work will elucidate this 3D-specific mechanosensing response.

Macrophages have increasingly been a subject of interest as targets for disease treatments. A meta-analysis reports more than 25 clinical trials targeting tumor-associated macrophages in a range of different cancer types [57]. In atherosclerosis, reducing macrophage mass within plaques is a promising strategy, as is increasing the numbers of anti-inflammatory macrophages and decreasing pro-inflammatory macrophages in damaged heart tissue after myocardial infarction [18, 58]. Depleting macrophages in models of skin wounding reduces hypertrophic scar formation [19]. As previously shown, targeting either macrophage or solid stress in glioblastoma improves outcomes [59–61]. Thus, understanding factors that contribute to macrophage expansion or reduction via a novel 3-D system could inform future treatment strategies.

Overall, this work demonstrates a novel platform to study previously unexplored aspects of macrophage mechanics. Because many diseases involve both altered macrophage content and altered mechanics, this model may elucidate new and targetable pathological interactions between macrophages and solid stress. Understanding how macrophages generate stress, and how they respond to external cues under chronic solid stress, will inform strategies to target or reprogram macrophages in the plethora of diseases that involve macrophage accumulation. This platform also has promise for screening macrophage-targeted drugs and is highly tunable to apply to a range of diseases.

Figure Captions

Fig. 1 Macrophage spheroids embedded in agarose form aggregates with sustained viability (**a**) Fraction dead cells 24h after seeding in agarose gels of varying concentration (**b**) Projections of macrophage spheroids 16 days after seeding show viable cells throughout the spheroid, in three different concentrations of agarose. Live cells are shown in green, dead cells shown in red, scale bar represents 50 μm. (**c**) Contour plots of the spheroid surface

Fig. 2 Agarose concentration modulates mechanical interactions and spheroid expansion. (**a**) Fluorescent imaging reveals that spheroids embedded in 0.5% agarose remain spherical, while those in 1% and 2% agarose become increasingly elongated and discoid. (**b**) Computational modeling visualizes the displacement field around expanding spheroids, with the greatest displacement seen in 0.5% agarose gels. Taken together, these results indicate that increasing agarose concentration restricts spheroid expansion and deformation, likely due to the increased mechanical rigidity restricting growth. The combined imaging and modeling approach provides visual evidence that agarose stiffness impacts spheroid morphology and expansion dynamics.

Fig. 3 Spheroid size varies with agarose stiffness and macrophage stimulation/polarization (**a**) Spheroid area, as quantified from brightfield images. (**b**) Representative images of maximum intensity projections of actin-stained spheroids (red)

Fig. 4 Immunofluorescent staining of spheroids sections for Ki67 and Piezo1. (**a**) Quantification and representative images of spheroid sections stained for Ki67(magenta) and Piezo1 (green). (**b**) Radial plots of

the normalized integrated staining intensity of representative spheroids, with a relative position of 1 representing the spheroid edge

Fig. 5 Macrophages show transcriptional response to both mechanical and chemical stimuli. qPCR analysis of genes related to proliferation and apoptosis (**a**), mechanosensitive ion channels (**b**), and macrophage polarization (**c**). Asterisks indicate comparisons which pass the false-discovery rate analysis

References

1. Park MD, Silvin A, Ginhoux F, Merad M (2022) Macrophages in health and disease. Cell 185:4259–4279. https://doi.org/10.1016/j.cell.2022.10.007

2. Locati M, Curtale G, Mantovani A (2020) Diversity, Mechanisms and Significance of Macrophage Plasticity. Annu Rev Pathol 15:123–147. https://doi.org/10.1146/annurev-pathmechdis-012418-012718

3. Yona S, Kim K-W, Wolf Y, Mildner A, Varol D, Breker M, Strauss-Ayali D, Viukov S, Guilliams M, Misharin A, Hume DA, Perlman H, Malissen B, Zelzer E, Jung S (2013) Fate mapping reveals origins and dynamics of monocytes and tissue macrophages under homeostasis. Immunity 38:79–91. https://doi.org/10.1016/j.immuni.2012.12.001

4. Davies LC, Rosas M, Jenkins SJ, Liao C-T, Scurr MJ, Brombacher F, Fraser DJ, Allen JE, Jones SA, Taylor PR (2013) Distinct bone marrow-derived and tissue resident macrophage-lineages proliferate at key stages during inflammation. Nat Commun 4:10.1038/ncomms2877. https://doi.org/10.1038/ncomms2877

5. Gerhardt T, Ley K (2015) Monocyte trafficking across the vessel wall. Cardiovascular Research 107:321–330. https://doi.org/10.1093/cvr/cvv147

6. Katkar G, Ghosh P (2023) Macrophage states: there's a method in the madness. Trends in Immunology 44:954–964. https://doi.org/10.1016/j.it.2023.10.006

7. Meli VS, Veerasubramanian PK, Atcha H, Reitz Z, Downing TL, Liu WF (2019) Biophysical regulation of macrophages in health and disease. Journal of Leukocyte Biology 106:283–299. https://doi.org/10.1002/JLB.MR0318-126R

8. Mittelheisser V, Gensbittel V, Bonati L, Li W, Tang L, Goetz JG (2024) Evidence and therapeutic implications of biomechanically regulated immunosurveillance in cancer and other diseases. Nat Nanotechnol 1–17. https://doi.org/10.1038/s41565-023-01535-8

9. Husain T, Abbott CR, Scott DJA, Gough MJ (1999) Macrophage accumulation within the cap of carotid atherosclerotic plaques is associated with the onset of cerebral ischemic events. Journal of Vascular Surgery 30:269–276. https://doi.org/10.1016/S0741-5214(99)70137-0

10. Montemurro N, Pahwa B, Tayal A, Shukla A, De Jesus Encarnacion M, Ramirez I, Nurmukhametov R, Chavda V, De Carlo A (2023) Macrophages in Recurrent Glioblastoma as a Prognostic Factor in the Synergistic System of the Tumor Microenvironment. Neurol Int 15:595–608. https://doi.org/10.3390/neurolint15020037

11. Yuan X, Zhang J, Li D, Mao Y, Mo F, Du W, Ma X (2017) Prognostic significance of tumor-associated macrophages in ovarian cancer: A meta-analysis. Gynecologic Oncology 147:181–187. https://doi.org/10.1016/j.ygyno.2017.07.007

12. Zhao X, Qu J, Sun Y, Wang J, Liu X, Wang F, Zhang H, Wang W, Ma X, Gao X, Zhang S (2017) Prognostic significance of tumor-associated macrophages in breast cancer: a meta-analysis of the literature. Oncotarget 8:30576–30586. https://doi.org/10.18632/oncotarget.15736

13. Kloepper J, Riedemann L, Amoozgar Z, Seano G, Susek K, Yu V, Dalvie N, Amelung RL, Datta M, Song JW, Askoxylakis V, Taylor JW, Lu-Emerson C, Batista A, Kirkpatrick ND, Jung K, Snuderl M, Muzikansky A, Stubenrauch KG, Krieter O, Wakimoto H, Xu L, Munn LL, Duda DG, Fukumura D, Batchelor TT, Jain RK (2016) Ang-2/VEGF bispecific antibody reprograms macrophages and resident microglia to anti-tumor phenotype and prolongs glioblastoma survival. Proc Natl Acad Sci U S A 113:4476–4481. https://doi.org/10.1073/pnas.1525360113

14. Datta M, Coussens LM, Nishikawa H, Hodi FS, Jain RK (2019) Reprogramming the Tumor Microenvironment to Improve Immunotherapy: Emerging Strategies and Combination Therapies. Am Soc Clin Oncol Educ Book 165–174. https://doi.org/10.1200/EDBK_237987

15. Andersen BM, Faust Akl C, Wheeler MA, Chiocca EA, Reardon DA, Quintana FJ (2021) Glial and myeloid heterogeneity in the brain tumour microenvironment. Nat Rev Cancer 21:786–802. https://doi.org/10.1038/s41568-021-00397-3

16. Rashidi A, Billingham LK, Zolp A, Chia T, Silvers C, Katz JL, Park CH, Delay S, Boland L, Geng Y, Markwell SM, Dmello C, Arrieta VA, Zilinger K, Jacob IM, Lopez-Rosas A, Hou D, Castro B, Steffens AM, McCortney K, Walshon JP, Flowers MS, Lin H, Wang H, Zhao J, Sonabend A, Zhang P, Ahmed AU, Brat DJ, Heiland DH, Lee-Chang C, Lesniak MS, Chandel NS, Miska J (2024) Myeloid cell-derived creatine in the hypoxic niche promotes glioblastoma growth. Cell Metabolism 36:62-77.e8. https://doi.org/10.1016/j.cmet.2023.11.013

17. Nia HT, Liu H, Seano G, Datta M, Jones D, Rahbari N, Incio J, Chauhan VP, Jung K, Martin JD, Askoxylakis V, Padera TP, Fukumura D, Boucher Y, Hornicek FJ, Grodzinsky AJ, Baish JW, Munn LL, Jain RK (2016) Solid stress and elastic energy as measures of tumour mechanopathology. Nat Biomed Eng 1:0004. https://doi.org/10.1038/s41551-016-0004

18. Simões FC, Cahill TJ, Kenyon A, Gavriouchkina D, Vieira JM, Sun X, Pezzolla D, Ravaud C, Masmanian E, Weinberger M, Mayes S, Lemieux ME, Barnette DN, Gunadasa-Rohling M, Williams RM, Greaves DR, Trinh LA, Fraser SE, Dallas SL, Choudhury RP, Sauka-Spengler T, Riley PR (2020) Macrophages directly contribute collagen to scar formation during zebrafish heart regeneration and mouse heart repair. Nat Commun 11:600. https://doi.org/10.1038/s41467-019-14263-2

19. Feng Y, Sun Z-L, Liu S-Y, Wu J-J, Zhao B-H, Lv G-Z, Du Y, Yu S, Yang M-L, Yuan F-L, Zhou X-J (2019) Direct and Indirect Roles of Macrophages in Hypertrophic Scar Formation. Frontiers in Physiology 10:

20. Adams S, Wuescher LM, Worth R, Yildirim-Ayan E (2019) Mechano-immunomodulation: Mechanoresponsive changes in macrophage activity and polarization. Ann Biomed Eng 47:2213–2231. https://doi.org/10.1007/s10439-019-02302-4

21. Fahy N, Menzel U, Alini M, Stoddart MJ (2019) Shear and Dynamic Compression Modulates the Inflammatory Phenotype of Human Monocytes in vitro. Front Immunol 10:383. https://doi.org/10.3389/fimmu.2019.00383

22. Grottkau BE, Noordin S, Shortkroff S, Schaffer JL, Thornhill TS, Spector M (2002) Effect of mechanical perturbation on the release of PGE2 by macrophages in vitro. Journal of Biomedical Materials Research 59:288–293. https://doi.org/10.1002/jbm.1244

23. Seneviratne AN, Cole JE, Goddard ME, Park I, Mohri Z, Sansom S, Udalova I, Krams R, Monaco C (2015) Low shear stress induces M1 macrophage polarization in murine thin-cap atherosclerotic plaques. Journal of Molecular and Cellular Cardiology 89:168–172. https://doi.org/10.1016/j.yjmcc.2015.10.034

24. Matheson LA, Maksym GN, Santerre JP, Labow RS (2006) Cyclic biaxial strain affects U937 macrophage-like morphology and enzymatic activities. Journal of Biomedical Materials Research Part A 76A:52–62. https://doi.org/10.1002/jbm.a.30448

25. Rho JY, Ashman RB, Turner CH (1993) Young's modulus of trabecular and cortical bone material: Ultrasonic and microtensile measurements. Journal of Biomechanics 26:111–119. https://doi.org/10.1016/0021-9290(93)90042-D

26. Budday S, Nay R, de Rooij R, Steinmann P, Wyrobek T, Ovaert TC, Kuhl E (2015) Mechanical properties of gray and white matter brain tissue by indentation. J Mech Behav Biomed Mater 46:318–330. https://doi.org/10.1016/j.jmbbm.2015.02.024

27. Hsieh JY, Keating MT, Smith TD, Meli VS, Botvinick EL, Liu WF (2019) Matrix crosslinking enhances macrophage adhesion, migration, and inflammatory activation. APL Bioeng 3:016103. https://doi.org/10.1063/1.5067301

28. Adlerz KM, Aranda-Espinoza H, Hayenga HN (2016) Substrate elasticity regulates the behavior of human monocyte-derived macrophages. Eur Biophys J 45:301–309. https://doi.org/10.1007/s00249-015-1096-8

29. Meli VS, Atcha H, Veerasubramanian PK, Nagalla RR, Luu TU, Chen EY, Guerrero-Juarez CF, Yamaga K, Pandori W, Hsieh JY, Downing TL, Fruman DA, Lodoen MB, Plikus MV, Wang W, Liu WF (2020) YAP-mediated mechanotransduction tunes the macrophage inflammatory response. Science Advances 6:eabb8471. https://doi.org/10.1126/sciadv.abb8471

30. Blakney AK, Swartzlander MD, Bryant SJ (2012) The effects of substrate stiffness on the in vitro activation of macrophages and in vivo host response to poly(ethylene glycol)-based hydrogels. J Biomed Mater Res A 100:1375–1386. https://doi.org/10.1002/jbm.a.34104

31. Dutta B, Goswami R, Rahaman SO (2020) TRPV4 Plays a Role in Matrix Stiffness-Induced Macrophage Polarization. Frontiers in Immunology 11:

32. Friedemann M, Kalbitzer L, Franz S, Moeller S, Schnabelrauch M, Simon J-C, Pompe T, Franke K (2017) Instructing Human Macrophage Polarization by Stiffness and Glycosaminoglycan Functionalization in 3D Collagen Networks. Advanced Healthcare Materials 6:1600967. https://doi.org/10.1002/adhm.201600967

33. Taufalele PV, Wang W, Simmons AJ, Southard-Smith AN, Chen B, Greenlee JD, King MR, Lau KS, Hassane DC, Bordeleau F, Reinhart-King CA (2023) Matrix stiffness enhances cancer-macrophage interactions and M2-like macrophage accumulation in the breast tumor microenvironment. Acta Biomater 163:365–377. https://doi.org/10.1016/j.actbio.2022.04.031

34. Larsen AMH, Kuczek DE, Kalvisa A, Siersbæk MS, Thorseth M-L, Johansen AZ, Carretta M, Grøntved L, Vang O, Madsen DH (2020) Collagen Density Modulates the Immunosuppressive Functions of Macrophages. J Immunol 205:1461–1472. https://doi.org/10.4049/jimmunol.1900789

35. Nia HT, Munn LL, Jain RK (2020) Physical traits of cancer. Science 370:eaaz0868. https://doi.org/10.1126/science.aaz0868

36. Stylianopoulos T, Martin JD, Chauhan VP, Jain SR, Diop-Frimpong B, Bardeesy N, Smith BL, Ferrone CR, Hornicek FJ, Boucher Y, Munn LL, Jain RK (2012) Causes, consequences, and remedies for growth-induced solid stress in murine and human tumors. Proc Natl Acad Sci U S A 109:15101–15108. https://doi.org/10.1073/pnas.1213353109

37. Nia HT, Datta M, Seano G, Huang P, Munn LL, Jain RK (2018) Quantifying solid stress and elastic energy from excised or in situ tumors. Nat Protoc 13:1091–1105. https://doi.org/10.1038/nprot.2018.020

38. Community SNP and M (2020) In vivo compression and imaging in the brain to measure the effects of solid stress. In: Springer Nature Protocols and Methods Community. http://protocolsmethods.springernature.com/users/419568-meenal-datta/posts/in-vivo-compression-and-imaging-in-the-brain-to-measure-the-effects-of-solid-stress. Accessed 28 Jul 2022

39. Zucca P, Fernandez-Lafuente R, Sanjust E (2016) Agarose and Its Derivatives as Supports for Enzyme Immobilization. Molecules 21:1577. https://doi.org/10.3390/molecules21111577

40. Suzawa Y, Kubo N, Iwai S, Yura Y, Ohgushi H, Akashi M (2015) Biomineral/Agarose Composite Gels Enhance Proliferation of Mesenchymal Stem Cells with Osteogenic Capability. Int J Mol Sci 16:14245–14258. https://doi.org/10.3390/ijms160614245

41. Normand V, Lootens DL, Amici E, Plucknett KP, Aymard P (2000) New Insight into Agarose Gel Mechanical Properties. Biomacromolecules 1:730–738. https://doi.org/10.1021/bm005583j

42. Berry MF, Engler AJ, Woo YJ, Pirolli TJ, Bish LT, Jayasankar V, Morine KJ, Gardner TJ, Discher DE, Sweeney HL (2006) Mesenchymal stem cell injection after myocardial infarction improves myocardial compliance. American Journal of Physiology-Heart and Circulatory Physiology 290:H2196–H2203. https://doi.org/10.1152/ajpheart.01017.2005

43. Hang J, Chen J, Zhang W, Yuan T, Xu Y, Zhou B (2021) Correlation between elastic modulus and clinical severity of pathological scars: a cross-sectional study. Sci Rep 11:23324. https://doi.org/10.1038/s41598-021-02730-0

44. Aykut B, Chen R, Kim JI, Wu D, Shadaloey SAA, Abengozar R, Preiss P, Saxena A, Pushalkar S, Leinwand J, Diskin B, Wang W, Werba G, Berman M, Lee SKB, Khodadadi-Jamayran A, Saxena D, Coetzee WA, Miller G (2020) Targeting Piezo1 unleashes innate immunity against cancer and infectious disease. Science Immunology 5:eabb5168. https://doi.org/10.1126/sciimmunol.abb5168

45. Janssen E, van den Dries K, Ventre M, Cambi A (2024) Mechanobiology of myeloid cells. Current Opinion in Cell Biology 86:102311. https://doi.org/10.1016/j.ceb.2023.102311

46. Atcha H, Jairaman A, Holt JR, Meli VS, Nagalla RR, Veerasubramanian PK, Brumm KT, Lim HE, Othy S, Cahalan MD, Pathak MM, Liu WF (2021) Mechanically activated ion channel Piezo1 modulates macrophage polarization and stiffness sensing. Nat Commun 12:3256. https://doi.org/10.1038/s41467-021-23482-5

47. Pathak MM, Nourse JL, Tran T, Hwe J, Arulmoli J, Le DTT, Bernardis E, Flanagan LA, Tombola F (2014) Stretch-activated ion channel Piezo1 directs lineage choice in human neural stem cells. Proceedings of the National Academy of Sciences 111:16148–16153. https://doi.org/10.1073/pnas.1409802111

48. Du H, Bartleson JM, Butenko S, Alonso V, Liu WF, Winer DA, Butte MJ (2022) Tuning immunity through tissue mechanotransduction. Nat Rev Immunol 1–15. https://doi.org/10.1038/s41577-022-00761-w

49. Michalick L, Kuebler WM (2020) TRPV4—A Missing Link Between Mechanosensation and Immunity. Frontiers in Immunology 11:

50. Datta M, Via LE, Kamoun WS, Liu C, Chen W, Seano G, Weiner DM, Schimel D, England K, Martin JD, Gao X, Xu L, Barry CE, Jain RK (2015) Anti-vascular endothelial growth factor treatment normalizes tuberculosis granuloma vasculature and improves small molecule delivery. Proceedings of the National Academy of Sciences 112:1827–1832. https://doi.org/10.1073/pnas.1424563112

51. Carey SP, Starchenko A, McGregor AL, Reinhart-King CA (2013) Leading malignant cells initiate collective epithelial cell invasion in a three-dimensional heterotypic tumor spheroid model. Clin Exp Metastasis 30:615–630. https://doi.org/10.1007/s10585-013-9565-x

52. Fang H, Pengal RA, Cao X, Ganesan LP, Wewers MD, Marsh CB, Tridandapani S (2004) Lipopolysaccharide-Induced Macrophage Inflammatory Response Is Regulated by SHIP1. The Journal of Immunology 173:360–366. https://doi.org/10.4049/jimmunol.173.1.360

53. Liu X, Wang N, Zhu Y, Yang Y, Chen X, Fan S, Chen Q, Zhou H, Zheng J (2016) Inhibition of Extracellular Calcium Influx Results in Enhanced IL-12 Production in LPS-Treated Murine Macrophages by Downregulation of the CaMKKβ-AMPK-SIRT1 Signaling Pathway. Mediators Inflamm 2016:6152713. https://doi.org/10.1155/2016/6152713

54. Müller E, Christopoulos PF, Halder S, Lunde A, Beraki K, Speth M, Øynebråten I, Corthay A (2017) Toll-Like Receptor Ligands and Interferon-γ Synergize for Induction of Antitumor M1 Macrophages. Frontiers in Immunology 8:

55. Tang Z, Wei X, Li T, Wu H, Xiao X, Hao Y, Li S, Hou W, Shi L, Li X, Guo Z (2021) Three-Dimensionally Printed Ti2448 With Low Stiffness Enhanced Angiogenesis and Osteogenesis by Regulating Macrophage Polarization via Piezo1/YAP Signaling Axis. Front Cell Dev Biol 9:750948. https://doi.org/10.3389/fcell.2021.750948

56. Yao M, Tijore A, Cheng D, Li JV, Hariharan A, Martinac B, Tran Van Nhieu G, Cox CD, Sheetz M (2022) Force- and cell state–dependent recruitment of Piezo1 drives focal adhesion dynamics and calcium entry. Science Advances 8:eabo1461. https://doi.org/10.1126/sciadv.abo1461

57. Wang H, Wang X, Zhang X, Xu W (2024) The promising role of tumor-associated macrophages in the treatment of cancer. Drug Resistance Updates 73:101041. https://doi.org/10.1016/j.drup.2023.101041

58. Sansonetti M, Al Soodi B, Thum T, Jung M (2024) Macrophage-based therapeutic approaches for cardiovascular diseases. Basic Res Cardiol 119:1–33. https://doi.org/10.1007/s00395-023-01027-9

59. Peterson TE, Kirkpatrick ND, Huang Y, Farrar CT, Marijt KA, Kloepper J, Datta M, Amoozgar Z, Seano G, Jung K, Kamoun WS, Vardam T, Snuderl M, Goveia J, Chatterjee S, Batista A, Muzikansky A, Leow CC, Xu L, Batchelor TT, Duda DG, Fukumura D, Jain RK (2016) Dual inhibition of Ang-2 and VEGF receptors normalizes tumor vasculature and prolongs survival in glioblastoma by altering macrophages. Proc Natl Acad Sci U S A 113:4470–4475. https://doi.org/flores-to

60. Flores-Toro JA, Luo D, Gopinath A, Sarkisian MR, Campbell JJ, Charo IF, Singh R, Schall TJ, Datta M, Jain RK, Mitchell DA, Harrison JK (2020) CCR2 inhibition reduces tumor myeloid cells and unmasks a checkpoint inhibitor effect to slow progression of resistant murine gliomas. Proc Natl Acad Sci U S A 117:1129–1138. https://doi.org/10.1073/pnas.1910856117

61. Datta M, Chatterjee S, Perez EM, Gritsch S, Roberge S, Duquette M, Chen IX, Naxerova K, Kumar AS, Ghosh M, Emblem KE, Ng MR, Ho WW, Kumar P, Krishnan S, Dong X, Speranza MC, Neagu MR, Iorgulescu JB, Huang RY, Youssef G, Reardon DA, Sharpe AH, Freeman GJ, Suvà ML, Xu L, Jain RK (2023) Losartan controls immune checkpoint blocker-induced edema and improves survival in glioblastoma mouse models. Proceedings of the National Academy of Sciences 120:e2219199120. https://doi.org/10.1073/pnas.2219199120

Figure 1

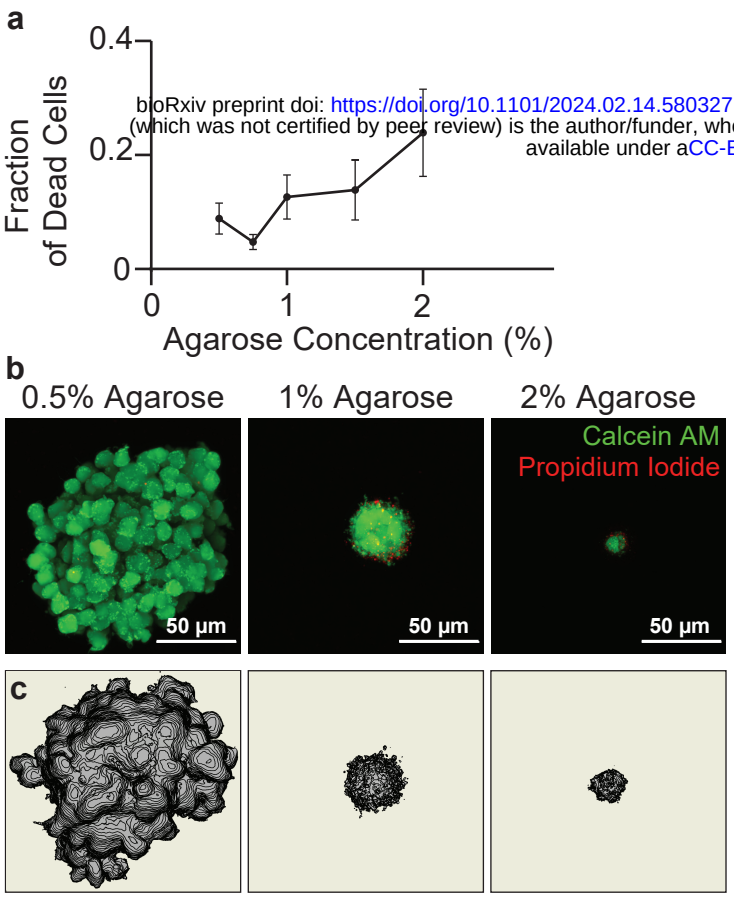

Figure 2

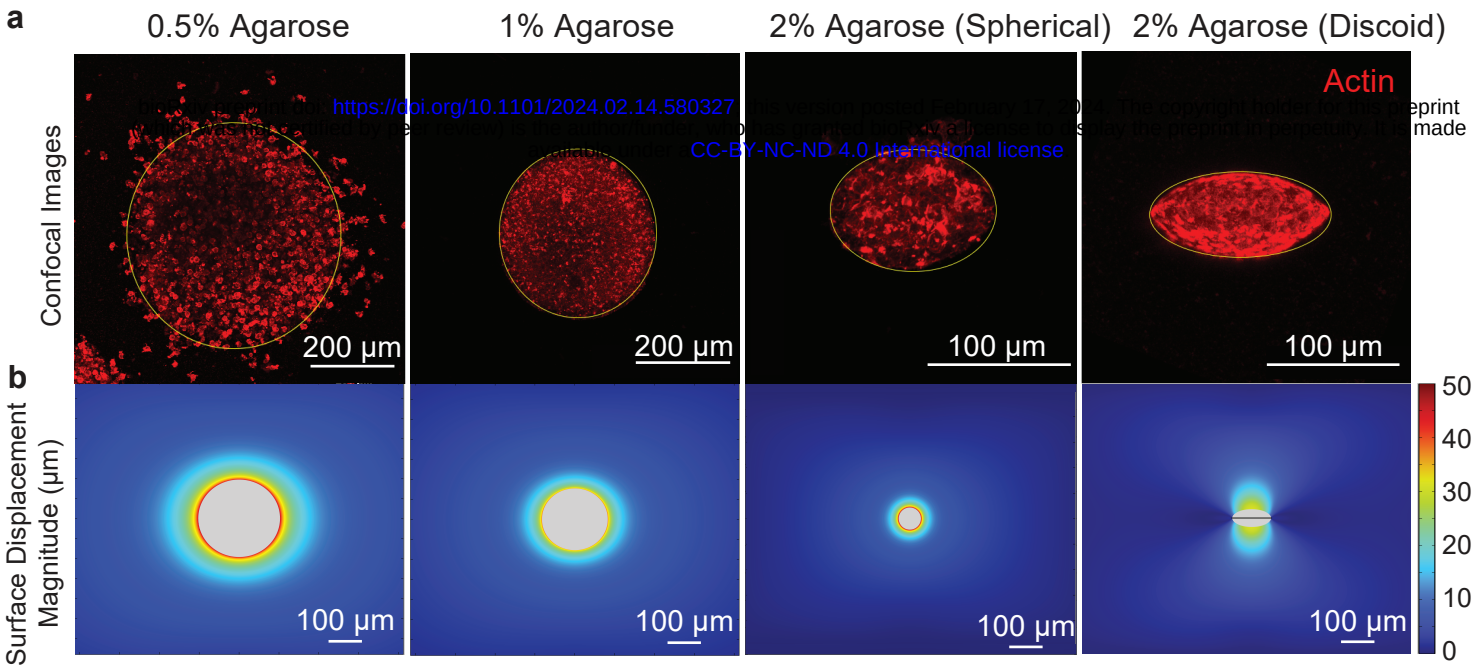

Figure 3

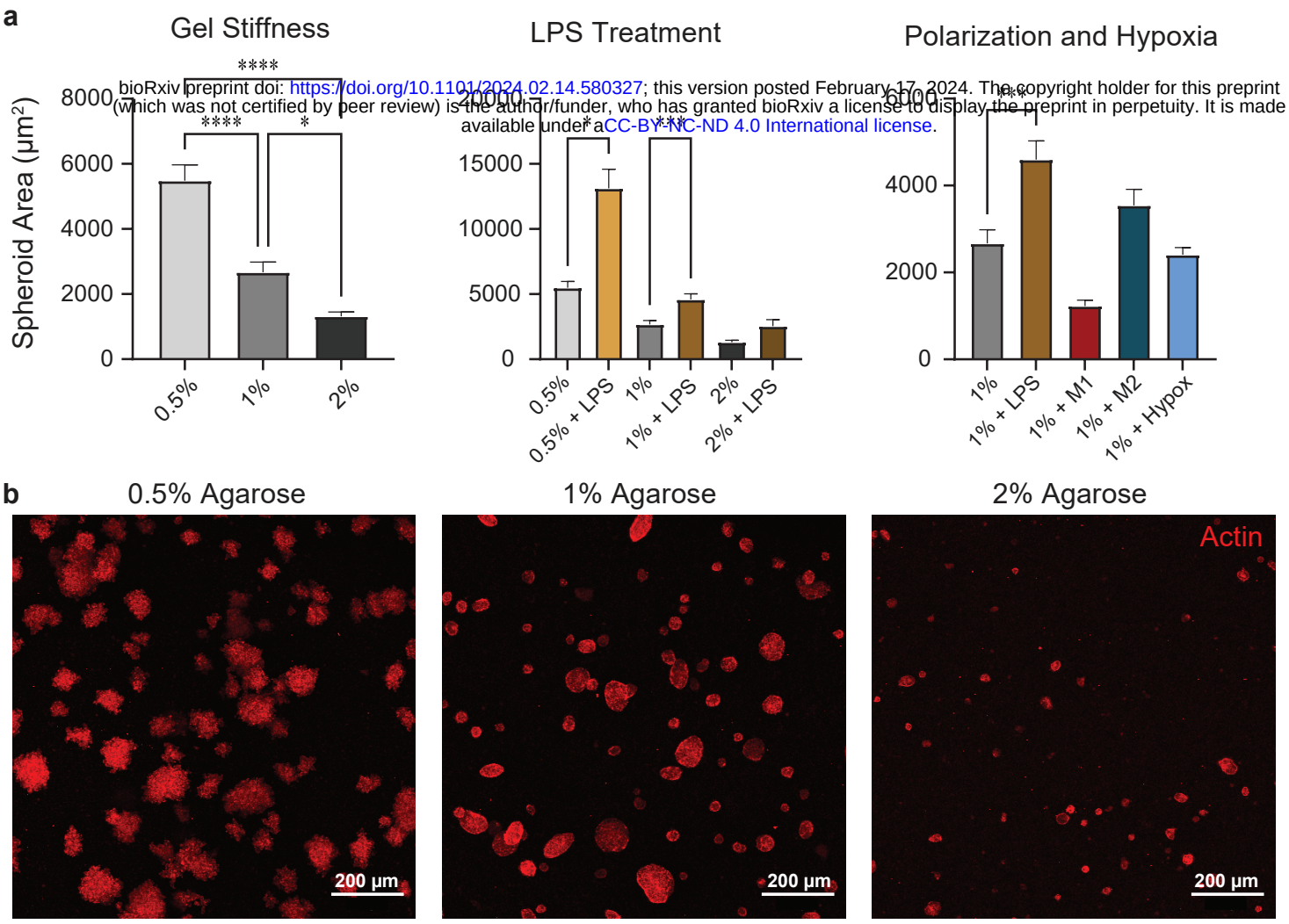

Figure 4

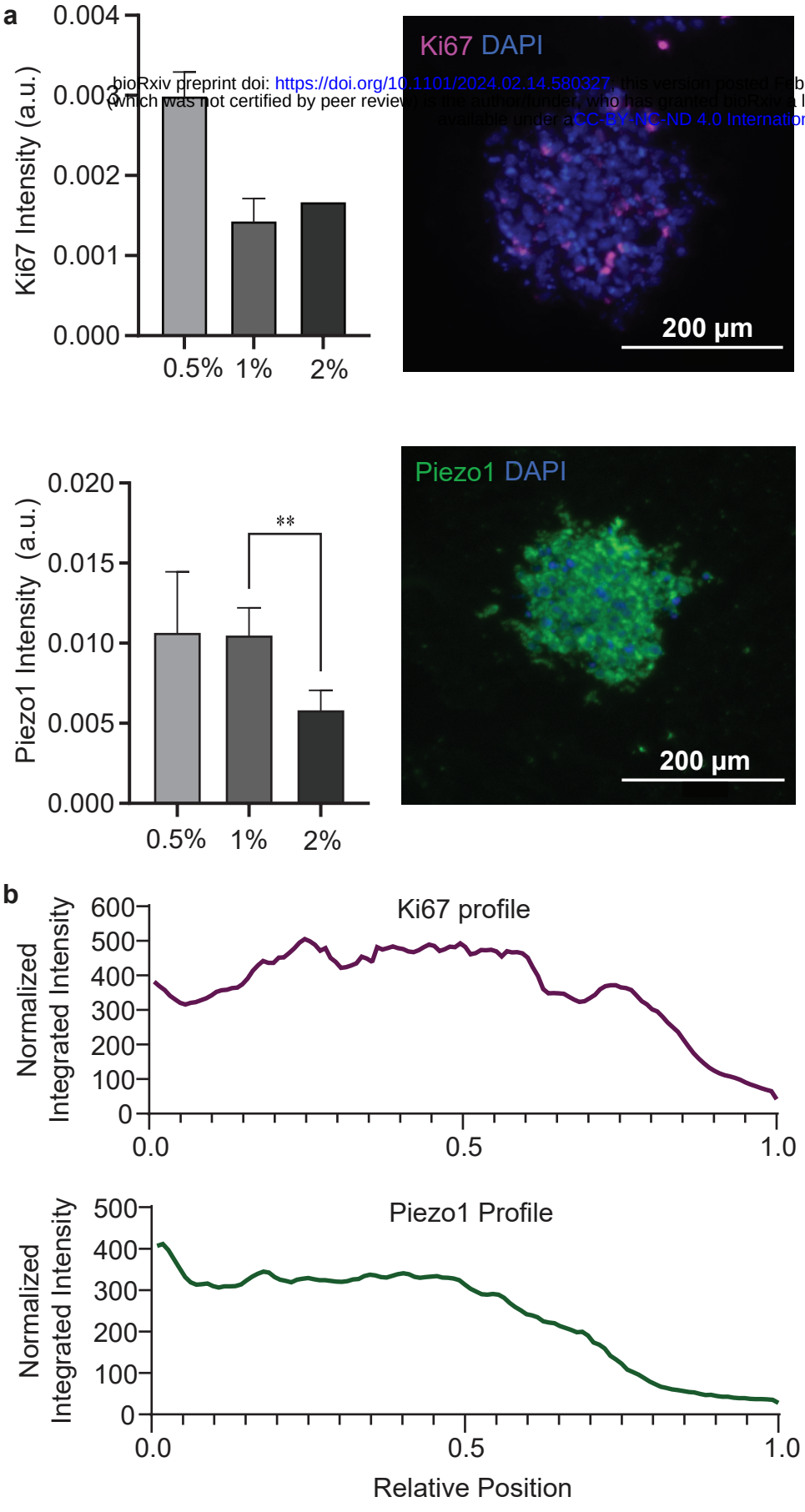

Figure 5